

# An Atom Faucet

W. Wohlleben<sup>a</sup>, F. Chevy, K. Madison, J. Dalibard,

Laboratoire Kastler Brossel<sup>b</sup>, Département de Physique de l'Ecole Normale Supérieure,  
 24 rue Lhomond, 75005 Paris, France

the date of receipt and acceptance should be inserted later

**Abstract.** We have constructed and modeled a simple and efficient source of slow atoms. From a background vapour loaded magneto-optical trap, a thin laser beam extracts a continuous jet of cold rubidium atoms. In this setup, the extraction column that is typical to leaking MOT systems is created without any optical parts placed inside the vacuum chamber. For detailed analysis, we present a simple 3D numerical simulation of the atomic motion in the presence of multiple saturating laser fields combined with an inhomogeneous magnetic field. At a pressure of  $P_{\text{Rb87}} = 1 \times 10^{-8}$  mbar, the moderate laser power of 10 mW per beam generates a jet of flux  $\Phi = 1.3 \times 10^8$  atoms/s with a mean velocity of 14 m/s and a divergence of  $< 20$  mrad.

**PACS.** 32.80.Lg Mechanical effects of light on atoms, molecules, and ions – 32.80.Pj Optical cooling of atoms; trapping

## 1 Introduction

Experiments on trapped cold atom clouds require in most cases high particle numbers and long trapping lifetimes. In order to restrict the lifetime limiting collisions with background gas, an ultra-high vacuum (UHV) environment is necessary. In turn, at these pressures a purely background vapour charged magneto-optical trap (VCMOT) is limited to very small atom numbers and long loading times and thus needs to be loaded by an additional jet of cold atoms.

As to the simplest possible cold atom sources, a laser-free velocity filter [1] is elegant, but its maximum flux can be greatly improved upon by adding a laser cooling stage.

The Zeeman slower is a widely used technique especially for light and thus thermally non capturable fast species. For heavier elements, one can accumulate atoms into a MOT in a vapour cell, with various strategies for subsequent transfer to a recapture MOT in the UHV cell. These strategies can be categorized into either a pulsed [2,3] or continuous transfer scheme. The latter category involves either a moving molasses [4] or a 'leaking MOT' scheme [5,6].

This paper presents the construction and numerical modeling of a cold atom jet whose flux is continuous, adjustable in a given direction, and velocity tunable. The device we present is based on an ordinary VCMOT. It captures and cools atoms from the low velocity part of the room temperature Maxwell-Boltzmann distribution in a high pressure cell of  $P \sim 10^{-8}$  mbar. From the center of

this source MOT, an additional pushing beam of  $\sim 1$  mm spot size extracts a continuous jet that is slow enough to be recaptured in a MOT in the UHV region. The jet passes through a tube that maintains the pressure differential between the two cells, and the atom number transfer between the two MOTs is found to be typically 50 % and as high as 60 % efficient.

The Atom Faucet is closely related to the LVIS [5] and the  $2\text{D}^+$ MOT [6]. The common concept which relates them in the 'leaking MOT' family is the creation of a thin extraction column in the center of the MOT where the radiation pressure is imbalanced and through which leaks a continuous jet of cold atoms. Operation in a continuous mode maximizes the mean flux up to a value ideally equal to the source trap capture rate. Since a leaking trap operates at a low trap density, once captured, an atom has much higher probability to leave the trap via the jet rather than undergoing a collision that expels it.

The LVIS and  $2\text{D}^+$ MOT place a mirror inside the vacuum for retroreflection of one of the MOT beams. By piercing a hole in this mirror, one creates a hollow retro-reflection beam, and the jet exits through the hole. By contrast, the Atom Faucet requires no optical parts inside the vacuum system. Here, we superimpose an additional collimated 'pushing beam' that pierces the extraction column through the MOT.

In these complex magneto-optical arrangements the behavior of the system is no longer intuitively obvious. On its way into the jet, a thermal atom undergoes subsequent phases of strong radiation pressure (capture from vapour), overdamped guidance to the magnetic field minimum (MOT molasses) and 1D strong radiation pressure with transverse 2D molasses cooling (extraction process).

<sup>a</sup> *Present address:* Max-Planck-Institut für Quantenoptik, 85748 Garching, Germany.

<sup>b</sup> Unité de Recherche de l'Ecole normale supérieure et de l'Université Pierre et Marie Curie, associée au CNRS.

Theoretical estimates for near-resonant atom traps concentrate either on the capture [7] or on the cooling [8]. We develop a simple and heuristic generalization of the semiclassical radiation pressure expression for the case of multiple saturating laser fields and inhomogeneous magnetic field. The new approach of integrating the atomic trajectory through both capture and cooling mechanisms (neglecting optical pumping and particle interaction) reproduces the parameter dependences of the Atom Faucet. The trajectories indicate the physical mechanisms of the 7-beam-interplay. However, the simplifications made to the Rubidium level scheme lead to an overestimation of the absolute value of the radiation pressure force and hence an overestimate for the capture velocity of the MOT.

This paper is organized as follows: In section 2 we give details on the experimental realization of the Atom Faucet. In section 3 we present the numerical model. Section 4 discusses the parameter dependences of the device in the experiment and in the simulations and finally in section 5 we compare this scheme to other vapour cell cold atom sources.

## 2 Experimental Realisation

The vacuum system consists of two glass cells separated vertically by 67 cm with a MOT aligned at the center of each cell. Using an appropriate pumping scheme and a differential pumping tube of diameter 5 mm and length 15 cm the pressure in the lower recapture cell is less than  $10^{-11}$  mbar while in the source cell it is  $\sim 10^{-8}$  mbar. We deduce the  $^{87}\text{Rb}$  pressure in the source cell from the resonant absorption of a multi-passed probe beam. A heated reservoir connected to the upper source cell supplies the Rubidium vapour.

A grating stabilized diode laser locked to the  $|5S_{1/2}, F = 2\rangle \rightarrow |5P_{3/2}, F = 3\rangle$  transition injects into three slave lasers, two for the source MOT and one for the recapture MOT. The Atom Faucet (see fig. 1) is based on a standard MOT configuration: two Anti-Helmholtz-coils maintain a magnetic field gradient of 15 G/cm along their axis, which is horizontal in this setup. A pair of axial beams with positive helicity counterpropagate along the axis of the coils and two mutually orthogonal pairs of radial beams with negative helicity counterpropagate in the symmetry plane of the coils. The radial beams are inclined by  $45^\circ$ . The radial trap beams have an 8 mm spot size and the axial beam 11 mm respectively, all clipped to a diameter of 1 inch by our quarterwaveplates. The axial beam carries 20 mW before retroreflection, and the radial beams each have 5 mW each before retroreflection. The repumping light on the  $|5S_{1/2}, F = 1\rangle \rightarrow |5P_{3/2}, F = 2\rangle$  transition from an independent grating stabilized laser is mixed only in the axial beam and has a power of  $\sim 5$  mW.

In addition to these trapping lasers, a permanent pushing beam on the  $|5S_{1/2}, F = 2\rangle \rightarrow |5P_{3/2}, F = 3\rangle$  transition with linear polarization [9] and optimal power of  $200 \mu\text{W}$  is aligned vertically onto the trap. It is focused to a waist of  $90 \mu\text{m}$  30 cm before entering the source cell such that it diverges to a size of 1.1 mm at the source trap and

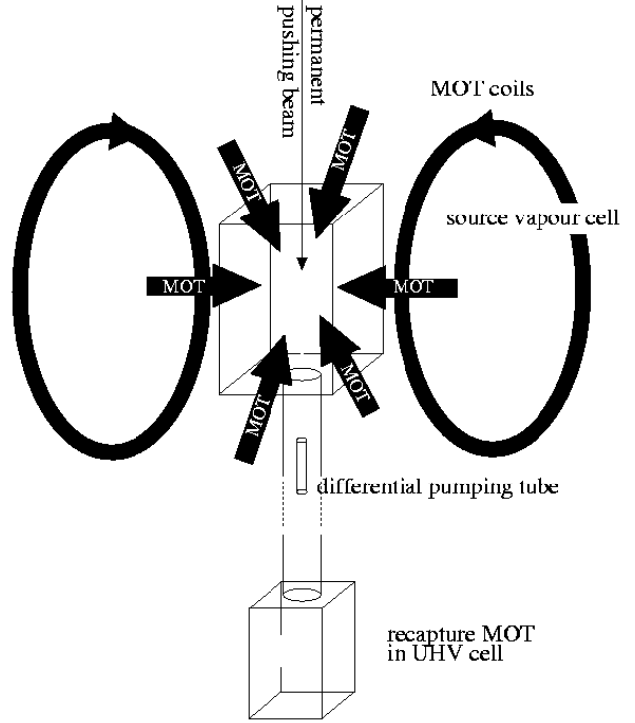


**Fig. 1.** The Atom Faucet setup (with the recapture MOT below). A permanent pushing beam with  $\sim 1$  mm spot size pierces an extraction column into an ordinary vapour charged MOT. The high pressure region is separated from the ultra-high-vacuum region by a differential pumping tube. The pressure in the source cell is monitored by the absorption of an additional multi-passed probe beam (not shown).

3.3 mm at the recapture trap. Its intensity at the center of the source MOT and detuning are comparable to those of the MOT beams and hence its radiation pressure is also comparable with the trapping forces in the MOT. Because of the divergence of the pushing beam, the intensity in the lower MOT is lower by a factor of 10. It decenters the recapture MOT by  $\simeq 1$  mm but does not destabilize it. Note that the pushing beam carries no repumping light, so that it acts on the atoms only where it intersects the MOT beams.

By studying the loading characteristics of the recapture MOT, we deduce the main features of the atom jet:

- When the recapture MOT is empty the initial recapture rate gives directly the recaptured flux since the density dependent intrinsic losses in the MOT are not yet important. The absolute number of atoms is determined using an absorption imaging technique.
- The time dependence of the recapture loading rate provides a measurement of the longitudinal velocity distribution of the jet. More precisely, by suddenly disinjecting the source MOT slave lasers and then recording the recapture filling rate via the fluorescence, the characteristics of the tail of the moving extraction column

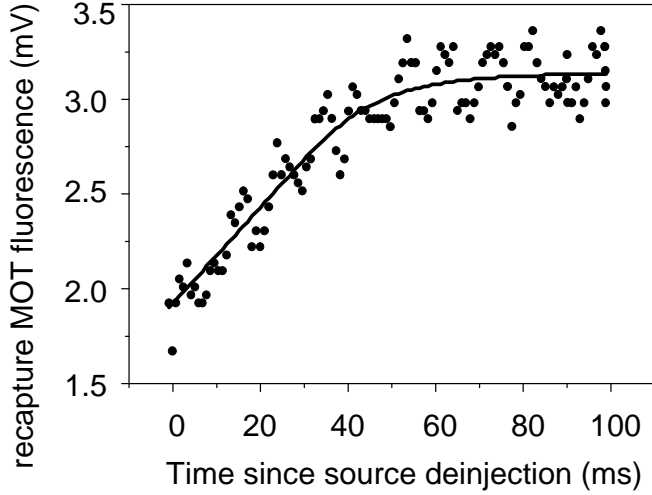


**Fig. 2.** Development of the fluorescence of the recapture trap (circles are photodiode signal) after sudden disinjection of the source MOT beams. The pushing beam is not changed in order to keep constant its influence on the lower trap fluorescence. The fit (solid line)  $\Phi(v) = \Phi_0 \times \exp(-(v - \bar{v})^2/2\delta v^2)$  with a Gaussian envelope for the jet velocity distribution yields  $v = 14 \pm 9$  m/s.

are measured. The jet transfer distance  $D = 67$  cm and the time delay  $T$  of the filling rate response gives the mean longitudinal velocity  $\bar{v} = D/T$  in the jet, and the time width  $\Delta t$  of this response gives access to the longitudinal velocity dispersion  $\delta v$  (see Fig. 2).

For the determination of the transfer efficiency, the loading rate of the source MOT is determined by its fluorescence and compared with the measured recapture flux. The fluorescence measurement is done at resonance and we assume full saturation of the transition under the influence of all six laser beams and thus a photon scattering rate of  $\Gamma/2$  photons/atom/second.

We observe a typical transfer efficiency of 50 % (see below). Since the radius of the recapture MOT beams is  $r = 5$  mm and the transfer distance is  $D = 67$  cm, less than 50 % of the atoms are emitted with a divergence larger than  $r/D \sim 10$  mrad.

### 3 Theoretical Description for Numerics

In order to model both the capture of the atoms from the vapor into the source MOT and the subsequent cooling and pushing processes, we have developed a numerical simulation which integrates the equation of motion for atoms chosen with random initial positions and velocities. We describe the atomic motion using classical dynamics. The action of the seven laser beams (6 MOT beams + 1 pushing beam) on an atom located at  $\mathbf{r}$  with velocity  $\mathbf{v}$  is taken into account through an average radiation force  $\mathbf{F}(\mathbf{r}, \mathbf{v})$ . We neglect any heating or diffusion caused by spontaneous emission.

The calculation of the semi-classical force acting on an atom in this multiple beam configuration is *a priori* very

complex. For simplicity, we model the atomic transition as a  $|g, J_g = 0\rangle \leftrightarrow |e, J_e = 1\rangle$  transition with frequency  $\hbar\omega_A$ , where  $|g\rangle$  and  $|e\rangle$  stand for the ground and excited state respectively. We denote  $\Gamma^{-1}$  the lifetime of  $e$ . Consider a single plane-wave beam with wave vector  $\mathbf{k}$ , detuning  $\delta = \omega_L - \omega_A$ , intensity  $I$ , and polarisation  $\sigma_{\pm}$  along the local magnetic field  $\mathbf{B}$  in  $\mathbf{r}$ . The radiation pressure force [10] reads

$$\mathbf{F} = \hbar\mathbf{k} \frac{\Gamma}{2} \frac{s(\mathbf{r}, \mathbf{v})}{1 + s(\mathbf{r}, \mathbf{v})} \quad (1)$$

where the saturation parameter is given by

$$s(\mathbf{r}, \mathbf{v}) = \frac{I}{I_{\text{sat}}} \frac{\Gamma^2}{\Gamma^2 + 4(\delta - \mathbf{k} \cdot \mathbf{v} \pm \mu B/\hbar)^2}.$$

$\mu$  is the magnetic moment associated with level  $|e\rangle$  and  $I_{\text{sat}}$  is the saturation intensity for the transition ( $I_{\text{sat}} = 1.62$  mW/cm<sup>2</sup> for the  $D_2$  resonance line in Rb). Still restricting our attention to a single traveling wave, we consider now the case where the light couples  $|g\rangle$  to two or three Zeeman sublevels  $|e_m\rangle$ . The calculation is in this case more involved since the solution of the optical Bloch equations requires the study of 16 coupled differential equations. A simple approximation is obtained in the low saturation limit ( $s \ll 1$ ):

$$\mathbf{F} = \hbar\mathbf{k} \frac{\Gamma}{2} \sum_{m=-1,0,1} s_m(\mathbf{r}, \mathbf{v}) \quad (2)$$

with

$$s_m = \frac{I_m}{I_{\text{sat}}} \frac{\Gamma^2}{\Gamma^2 + 4(\delta - \mathbf{k} \cdot \mathbf{v} + m\mu B/\hbar)^2}$$

and where  $I_m$  is the intensity of the laser wave driving the  $|g\rangle \leftrightarrow |e_m\rangle$  transition. We can sum up the three forces associated with the three possible transitions, each calculated with the proper detuning taking into account the Zeeman effect.

Still working in the low intensity limit, we can generalize eq. (2) to the case where  $N$  laser beams with wave vectors  $\mathbf{k}_j$  and detunings  $\delta_j$ , ( $j = 1, \dots, N$ ) are present. The force then reads

$$\mathbf{F} = \sum_j \hbar\mathbf{k}_j \frac{\Gamma}{2} \sum_{m=-1,0,1} s_{j,m}(\mathbf{r}, \mathbf{v}) \quad (3)$$

with

$$s_{j,m} = \frac{I_{j,m}}{I_{\text{sat}}} \frac{\Gamma^2}{\Gamma^2 + 4(\delta_j - \mathbf{k}_j \cdot \mathbf{v} + m\mu B/\hbar)^2}$$

Note that in establishing eq. (3) we have taken the spatial average of the radiative force over a cell of size  $\lambda = 2\pi/k$ , neglecting thus all interference terms varying as  $i(\mathbf{k}_j - \mathbf{k}_{j'}) \cdot \mathbf{r}$ . We therefore neglect any effect of the dipole force associated with the light intensity gradients on the wavelength scale. This is justified in the case of a leaking MOT since the associated dipole potential wells are much less deep than the expected residual energy of the atoms before extraction.

At the center of the capture MOT, we can no longer neglect inter-beam saturation effects since the saturation parameter for each of the 7 beams is equally  $\sim 1/7$ . In principle, accounting for this saturation effect requires a step-by-step numerical integration of the 16 coupled Bloch optical equations (for a  $|g, J_g = 0\rangle \leftrightarrow |e, J_e = 1\rangle$  transition), as the atom moves in the total electric field resulting from the interference of all the laser beams present in the experiment. Such a calculation is unfortunately much too computationally intensive to lead to interesting predictions for our Atom Faucet in a reasonable time. We therefore decided to turn to a heuristic and approximate expression for the force, demanding:

- In the case of a single traveling wave,  $\sigma_{\pm}$  polarized along the magnetic field, we should recover expression (1).
- In the low intensity limit, the force should simplify to expression (3).
- The magnitude of the force should never exceed  $\hbar k \Gamma/2$ , which is the maximal radiation pressure force in a single plane wave.

There are of course an infinite number of expressions which fulfill these three conditions. We have taken the simplest one:

$$\mathbf{F} = \sum_i \hbar \mathbf{k}_i \frac{\Gamma}{2} \frac{\sum_m s_{i,m}}{1 + \sum_{j,m} s_{j,m}} \quad (4)$$

with partial saturation parameters  $s_{j,m}$  as defined in eq. (3). This equation is the generalization of the heuristic expression used by Phillips and co-workers [8] to account for saturation effects in an optical molasses.

In the simulation, the MOT beams are chosen to have Gaussian profiles truncated to the diameter of the quarterwaveplates. Also they are chosen to be equally strong with a central intensity of  $5 I_{\text{sat}}$  and to have the proper polarizations and directions. The pushing beam's intensity is of the same order. We assume that because of optical pumping into the lower hyperfine ground state, an atom sees no forces when it is out of the repumper light mixed in the axial beams. Finally, the magnetic quadrupole field is  $\mathbf{B}(\mathbf{x}) = b'(-2x, y, z)$ .

In the simulation the initial position of each atom is chosen on one of the cell windows following a uniform spatial distribution. The initial velocity is given by a Maxwell Boltzmann distribution for  $T = 300$  K. The trajectory is then integrated using a Runge-Kutta method. From these trajectories (see fig. 3), one obtains a probability for an atom to be captured and transferred into the jet, as well as the jet's characteristics: velocity distribution, divergence, and total flux. The absolute flux of the simulated jet is calibrated using the real number of atoms emitted per unit time and per unit surface of the cell at a pressure  $P$  which is  $P/\sqrt{2\pi m k_B T}$  [11, 12].

The simulation neglects interaction effects like collisions and multiple light scattering. The validity of the linear scaling with pressure is limited to the low pressure regime ( $P < 10^{-7}$  mbar) where the characteristic extraction time of  $\simeq 20$  ms is shorter than the collision time, which is in turn of the order of the trap lifetime.

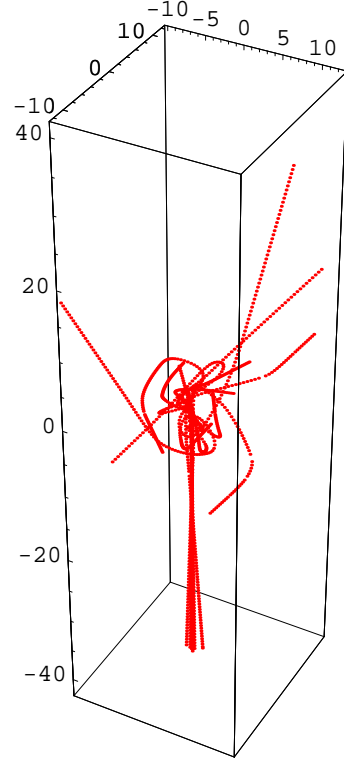


**Fig. 3.** Some simulated trajectories of atoms in the VCMOT + pushing beam light field that are captured and transferred to the jet (distances in mm).

## 4 Results

Inspecting qualitatively the trajectories, we find that an atom that enters the beam intersection is first decelerated by radiation pressure on a distance much smaller than the trapping beam radius. It then slowly moves to the center of the trap where it enters the extraction column. The final transverse cooling of the jet takes place during extraction, so that the divergence of the jet grows if the extraction happens too fast. We believe that this is the principal loss mechanism of any leaking MOT system, which have in common an extraction column and a transverse molasses provided by the trapping beams.

### 4.1 Total Flux

For a typical choice of parameters, the simulation finds 90 % transfer from the source MOT through the differential pumping tube to the recapture MOT. The remaining 10 % of the atoms leave the source at a divergence too large to be recaptured and are lost. Experimentally, we have achieved a transfer efficiency of at most  $60 \pm 10$  %. This value is most probably limited by the differential pumping tube diameter.

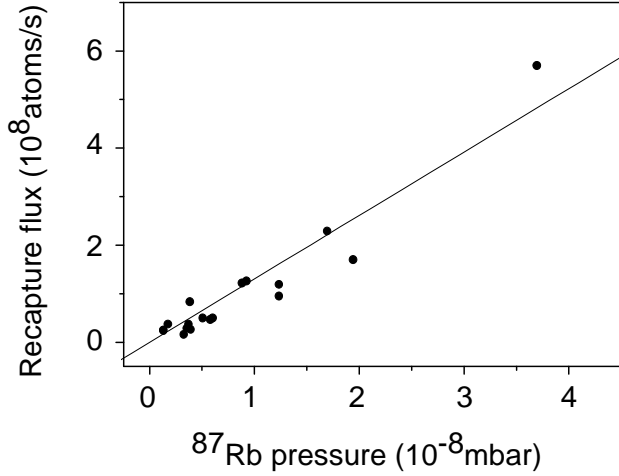


**Fig. 4.** Recaptured flux versus source cell pressure. The linear fit yields  $\Phi_{\text{exp}}^{\text{jet}} = 1.3 \pm 0.2 \times 10^8 \text{ atoms/s} \times P_{\text{Rb87}}(10^{-8} \text{ mbar})$ .

Concerning the total flux, we explored the pressure regime of  $10^{-9} < P < 4 \times 10^{-8} \text{ mbar}$  and found no deviation from a linear dependence (see fig. 4)

$$\Phi_{\text{exp}}^{\text{jet}} = 1.3 \pm 0.4 \times 10^8 \text{ atoms/s} \times P_{\text{Rb87}}(10^{-8} \text{ mbar}).$$

The uncertainty primarily comes from the atom number determination in the recapture MOT by absorption imaging. Deviation from linear scaling with pressure is to be expected when the collision time with background gas becomes of the order of the typical extraction time from the MOT center into the differential pumping tube. This will be the case for  $P_{\text{Rb87}} \geq 10^{-7} \text{ mbar}$ .

In comparison we found that the simulation overestimates the capture velocity of the MOT, so that we need to calibrate its predictions. Therefore we simulate a pure MOT without pushing beam and compare the predicted capture rate of

$$\tau_{\text{sim}}^{\text{MOT}} = 13 \times 10^8 \text{ atoms/s} \times P_{\text{Rb87}}(10^{-8} \text{ mbar})$$

with the value we measured in the initial regime of linear growth of the vapour charged source MOT,

$$\tau_{\text{exp}}^{\text{MOT}} = 2.5 \pm 0.6 \times 10^8 \text{ atoms/s} \times P_{\text{Rb87}}(10^{-8} \text{ mbar})$$

We believe that the disagreement between these two results corresponds to an overestimation of the source MOT capture velocity  $v_c$ . Since the number of atoms captured in a VCMOT varies as  $v_c^4$ , our simple model overestimates  $v_c$  by  $(13/2.5)^{1/4} \sim 1.5$ . In the graphs 5,6,7, we normalize the absolute value of the flux and concentrate on its variation with system parameters.

**Simulated VCMOT Optimisation.** Using the simulation of a pure MOT without pushing beam, we can readily find the parameters which optimise the capture rate from the background vapour. The total laser power is taken to be 20 mW, equally distributed among three beams which are

then retroreflected. We calculate an optimal detuning of  $-3 \Gamma$ . The capture rate is divided by more than 2 when the detuning is beyond  $-4.5 \Gamma$  or smaller than  $-1.5 \Gamma$ . This is the typical MOT operation range. The magnetic gradient seems to have little influence as long as it is between 8 and 20 G/cm.

It is particularly helpful to calculate the optimal beam waist for a given laser power since in the optical setup this parameter is tiresome to change and demands subsequent trap realignment. In our case, a 9 mm spot size gives the best simulated capture rate, with half maximum values at 4 mm and 16 mm. For a fixed laser power, having a large intersection volume is preferable to increasing the saturation beyond  $\sim 4 I_{\text{sat}}$ . The experiment uses an 8 mm spot size, and the optimum parameters do not change significantly if the retroreflection loss of 20 % is included. Finally, the simulation reproduces the smoothly decreasing slope of the capture rate versus the MOT beam power of ref [7].

## 4.2 Pushing Beam Parameters

We now add the thin pushing beam to the MOT light field. Doing so does not modify the optimal parameters of the capture MOT, neither in experiment nor in the simulation. Remember that the volume affected by the thin beam is very small compared to the total capture volume of the source MOT. We investigate the influence of pushing beam power, detuning, and size on the atomic jet emerging from the MOT. The following discussion shall directly combine experimental findings and the results from the theoretical model.

**Power.** For very low pushing beam power the trap is de-centered but not yet leaking. At  $P_{\text{push}} = 80 \mu\text{W}$  (corresponding to a pushing beam intensity 1/4 of a MOT beam intensity), the flux increases sharply and then falls off with increasing power (see fig. 5). The simulation predicts exactly the same critical power, without adjustable parameters (see fig. 5). The decrease at higher power can be understood if one examines the simulated divergence of the atomic jet, which grows with increasing pushing beam power. This effect is attributed to an insufficient short transverse cooling time due to the strong acceleration (see discussion below). Experimentally the jet velocity is deduced from measurements like fig. 2. With increasing pushing beam power it grows from 12 to 15 m/s with an average width of 10 m/s. In the simulation, we find a smaller width of 1 m/s. This discrepancy is probably due to the fact that we have completely neglected the heating due to spontaneous emission. The longitudinal velocity width is larger than that of the LVIS or 2D MOT; however, for the purpose of loading a recapture MOT the velocity width does not matter.

**Detuning.** The complex behaviour of the flux on the pushing beam detuning ( $\delta_{\text{push}}$ ) is qualitatively very well reproduced by the simulation (see figs. 6 and 7). If the pushing

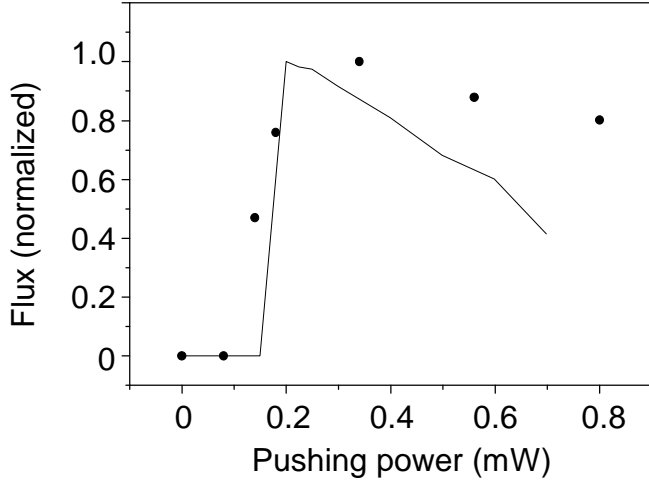


**Fig. 5.** Dependence of the atomic flux on the pushing beam power. Flux is normalized, see text. The dots are experimental, the solid line is simulation.

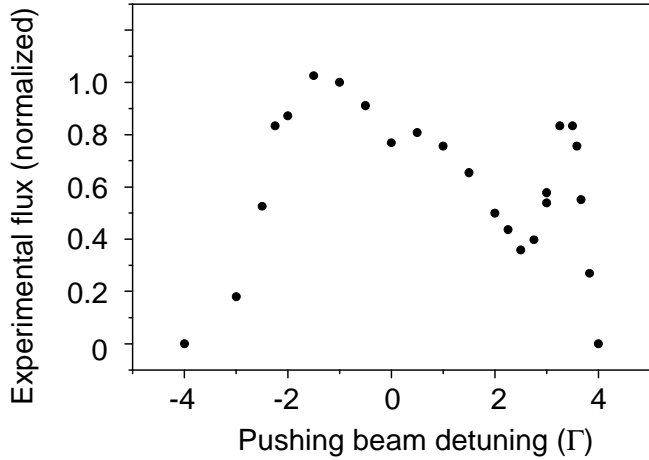


**Fig. 6.** Dependence of the atomic flux on the pushing beam detuning. The flux is normalized as indicated in the text.

beam detuning is negative and exceeds the MOT beam detuning  $|\delta_{\text{push}}| > |\delta_{\text{MOT}}|$ , the trap is decentered, but not yet leaking. Remember that the intensity of the pushing beam is about the same as for the MOT beams, so that as the detuning is increased the pushing radiation pressure becomes weaker than the trapping pressure. With zero or small blue detuning, atoms are resonantly accelerated, and their extraction is too fast to allow for efficient transverse cooling. These atoms leave at high divergence and are lost. Generally the simulation finds a 1 : 1 correlation of extraction time (flight time  $\sim 10$  ms from the center of the trap to the depumping region) with divergence. Clearly, transverse cooling takes a certain time, and if the extraction acceleration is too strong, losses due to a high beam divergence are inevitable.

For a blue detuning of the pushing beam such that  $\delta_{\text{push}} \simeq |\delta_{\text{MOT}}|$ , a prominent peak in the flux appears in both the experiment and the simulation. To interpret this result we use the model of a  $|g, J_g = 0\rangle \leftrightarrow |e, J_e = 1\rangle$  transition in a one dimensional magneto-optical trap (the

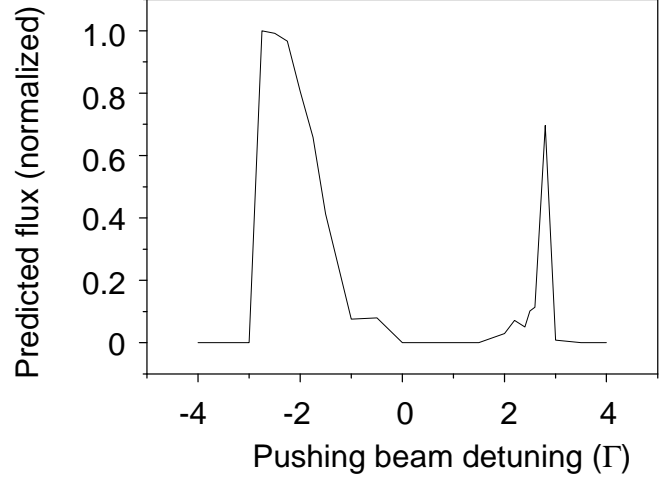


**Fig. 7.** Simulation of the dependence of the atomic flux on pushing beam detuning. The flux is normalized as indicated in the text.

actual beam inclination and polarisation make the situation a bit more complicated). For an atom traveling downwards in the extraction column, the  $|e, m = -1\rangle$  level approaches the MOT beam resonance at negative detuning. At the same time, the  $|e, m = +1\rangle$  level approaches the pushing beam resonance at positive detuning. When  $\delta_{\text{push}} \simeq |\delta_{\text{MOT}}|$ , the accelerating pushing beam and the decelerating MOT beams stay equally close to resonance throughout the extraction, and the atoms leave slowly. The extraction time is  $\sim 8$  ms and the atoms are cooled transversely leading to a large recapture flux in the lower MOT. Finally if  $\delta_{\text{push}} > |\delta_{\text{MOT}}|$ , the detuning of the  $|e, m = -1\rangle$  level from the recentering MOT light is always less than the detuning of the  $|e, m = +1\rangle$  level from the pushing beam light, and so the trap is decentered but not destabilized (analogous to the behaviour at a large red detuning).

**Complementary Numerical Study: Waist.** With a very small pushing beam size  $< 0.4$  mm atoms drift out of the extraction column and are decelerated. They are recycled forever or leave the trap with high divergence. For a large spot size of  $> 1.5$  mm atoms are not all extracted from the center and so many are not cooled sufficiently transversely. Both cases induce losses.

## 5 Comparison and Conclusion

Certainly, there are other techniques for the directed transfer of cold atoms from a VCMOT into a jet. A moving molasses launch [2] provides a rather cold beam but low flux. A pulsed MOT launched by a resonant beam push is heated in the absence of transverse cooling beams [3]. During the launch  $\sim \sqrt{1000}$  photons are spontaneously emitted into the transverse plane, while in continuous schemes there is transverse cooling during extraction. As a result

there is then no need for magnetic guiding [13], to achieve an elevated transfer efficiency.

Continuous schemes suffer less from interparticle interactions, since the steady state source cloud stays small. Leaking MOTs therefore accumulate atoms with the initial capture rate of the MOT. The Atom Faucet provides a 50 % transfer efficiency from first capture, through the differential pumping tube, and to a recapture MOT in an UHV cell. It creates an extraction column that is typical of leaking MOT systems with a flexible design and without optical parts inside the vacuum chamber.

The flux of  $\Phi = 1 \times 10^8$  atoms/s at a background vapour pressure of  $P_{\text{Rb87}} = 7.6 \times 10^{-9}$  mbar is equal to that of the low power version of the LVIS in [6] and superior to the 2D<sup>+</sup> MOT in this pressure region. The later design in turn provides very high flux at high pressure, since it minimizes the source trap density. We did not explore pressures that were incompatible with the UHV requirements in our recapture cell and found no deviation from the linear scaling of the flux with pressure up to pressures of  $4 \times 10^{-8}$  mbar. Essentially, the Atom Faucet transplants to a MOT at  $10^{-11}$  mbar the loading rate of a MOT at few  $10^{-8}$  mbar.

We have also presented a 3D simulation of the atomic motion in multiple laser fields with an inhomogeneous magnetic field, neglecting interactions and fluctuations. We find that the transverse cooling *inside* the extraction column turns out to be a crucial element for the satisfactory performance of leaking MOT atom sources. Our simulation overestimates the capture rate, but predicts well the measured parameter dependences. Moreover, it is readily adapted to an arbitrary laser and *B*-field configuration.

We are indebted to F. Pereira dos Santos for coming up with the child's name and to the ENS Laser Cooling Group for helpful discussions. This work was partially supported by CNRS, Collège de France, DRET, DRED, and EC (TMR network ERB FMRX-CT96-0002). This material is based upon work supported by the North Atlantic Treaty Organisation under an NSF-NATO grant awarded to K.M. in 1999. W.W. gratefully acknowledges support by the Studienstiftung des deutschen Volkes and the DAAD.

*Note added: After this work was completed, we became aware that a similar setup has been successfully achieved in Napoli, in the group of Prof. Tino.*

## References

1. B. Ghaffari, J. M. Gerton, W. L. McAlexander, K. E. Strecker, D. M. Homan and R. G. Hulet, Phys. Rev. A **60**, 3878 (1999)
2. S. Weyers, E. Auccouturier, C. Valentin and N. Dimarcq, Optics Comm. **143**, 30 (1997)
3. J.J. Arlt, O. Maragó, S. Webster, S. Hopkins and C. J. Foot, Optics Comm. **157**, 303 (1998)
4. H. Chen and E. Riis, Appl. Phys. B **70**, 665 (2000)
5. Z.T. Lu, K. L. Corwin, M. J. Renn, M. H. Anderson, E. A. Cornell and C. E. Wieman, Phys. Rev. Lett. **77**, 3331 (1996)
6. K. Dieckmann, R. J. C. Spreeuw, M. Weidemüller and J. T. M. Walraven, Phys. Rev. A **58**, 3891 (1998)
7. K. Lindquist, M. Stephens and C. Wieman, Phys. Rev. A **46**, 4082 (1992)
8. P.D. Lett, W. D. Phillips, S. L. Rolston, C. E. Tanner, R. N. Watts and C. I. Westbrook, J. Opt. Soc. Am B **6**, 2084 (1989)
9. We checked that neither in experiment nor in simulation does the direction of the linear polarization have any effect.
10. C. Cohen-Tannoudji, J. Dupont-Roc and G. Grynberg, *Atom-Photon Interactions, Basic Processes* (Wiley 1992).
11. F. Reif, *Fundamentals of statistical and thermal physics* (McGraw-Hill, New York, 1965).
12. In order to increase the efficiency of the simulation we only evolve atoms with an initial velocity lower than  $v_{\text{max}} = 45$  m/s. We checked that atoms with a larger velocity cannot be captured in the MOT, whatever the direction of their initial velocity.
13. C.J. Myatt, N. R. Newbury, R. W. Ghrist, S. Loutzenhiser and C. E. Wieman, Opt. Lett. **21**, 290 (1995)